

New Orbit Propagator to Be Used in Orbital Debris Evolutionary Models

Narumi, Tomohiro

Department of Aeronautics and Astronautics, Kyushu University

Hanada, Toshiya

Department of Aeronautics and Astronautics, Kyushu University

<https://hdl.handle.net/2324/8725>

出版情報：九州大学工学紀要. 67 (4), pp.235-254, 2007-12-20. 九州大学大学院工学研究院
バージョン：
権利関係：

New Orbit Propagator to Be Used in Orbital Debris Evolutionary Models

by

Tomohiro NARUMI* and Toshiya HANADA**

(Received November 5, 2007)

Abstract

An orbital environment debris evolutionary model for low Earth orbit has been developed at Kyushu University. A fast orbit propagator is essentially needed in such an evolutionary model because the number of space debris larger than 1 cm in low earth orbit is very large and it takes much time to compute long-term orbital changes of space debris. The effects of orbital perturbations are investigated for hundreds of years, and the rate of change in orbital elements were invented by earlier publications. New expressions of the rate of change in orbital elements are presented to account for gravitational forces of the Sun and Moon. This paper analyzes the long-term effects of orbital perturbations based on the new analytic models of third body forces and conventional analytical models of atmospheric drag, solar radiation pressure, and zonal harmonics. Some results are shown that can predict the changes of the orbit. The models shown in this paper will be useful for long-term calculation of the satellite orbits.

Keywords: Space debris, Satellite, Orbit, Propagator

1. Introduction

The population of artificial objects in space is growing continuously, with around 96% of the more than 9,000 cataloged objects in orbit being debris. Spent rocket bodies and inactive payloads occupy the most on-orbit population in mass and number. Particles from centimeters through millimeters in size, which are difficult to detect by ground facilities, are hazardous and may destroy space structures that are not sufficiently protected. One breakup in space can create several hundred or more fragments that are potential hazards to other spacecraft. It is necessary not only to avoid collisions between operating spacecraft and orbital debris but also to stop degradation of the orbital environment. Study and long-term prediction of the orbital debris environment in low-Earth orbit (LEO) are especially urgent needs for secure and safe human space development and exploration. Kyushu University has developed an orbital debris environmental evolutionary model in LEO. In the model, a fast orbit propagator is especially needed because the number of space debris larger than 1 cm in LEO is very large and it takes much time to compute the long-term orbital evolutions

* Graduate Student, Department of Aeronautics and Astronautics

** Associate Professor, Department of Aeronautics and Astronautics

of all orbital debris observed.

The studies of the general orbit perturbation techniques have been continued for hundreds of years by many scientists since Newton studied the Moon's motion. Nowadays, the innovation of intelligent technology enables us to calculate orbits of satellites numerically with computers. However, analytical solutions have the merit that can calculate long-term evolution of an orbit with a long step size (e.g., 5-day), and they make it easy to understand how the orbit evolves and provides deep insight on orbit perturbations.

In chapter 2, a new analytical model of gravitational forces of the Sun and Moon are presented that can be applied to satellites of arbitrary specifications. In chapter 3, a new analytical model of atmospheric drag is introduced. In chapter 4, the results of comparisons between the conventional propagator and the new propagator are shown. The present work analyzes the long-term effects of perturbations of the orbital elements (semi-major axis a , eccentricity e , inclination i , right ascension of ascending node Ω , argument of perigee ω and mean anomaly M) faster and more accurate than conventional methods.

2. Gravitational Perturbations

Luni-Solar perturbations of the orbit of an earth satellite are not negligible because of the large attraction forces. Therefore, the effects of the gravitational perturbations of the Sun and Moon were investigated by many mathematicians and scientists. According to Cook³⁾, the first paper was published by Spitzer²³⁾ using only the first terms of the Hill-Brown lunar theory. In the second, paper, Kozai¹⁷⁾ introduced the disturbing function due to the Sun and Moon including secular and long period terms. After that, various efforts by Moe¹⁸⁾, Geyling¹³⁾, Musen^{19,20,21)}, and Cook improved the disturbing function. In this section, the new perturbing functions due to the Sun and Moon is shown which is derived strictly to second order of the distance.

2.1 Perturbation due to the i -th body

The perturbing function due to the i -th body, U_i can be expressed by

$$U_i = \frac{Gm_i}{|\mathbf{r}_i - \mathbf{r}|} - \frac{Gm_i}{r_i^2} (\mathbf{r} \cdot \mathbf{r}) \quad (2.1)$$

where G represents the Earth's gravitational constant, m_i is the mass of the i -th body, \mathbf{r}_i is the geocentric position vector of the i -th body, and \mathbf{r} is the geocentric position vector of the satellite.

If $\mathbf{r}_i \gg \mathbf{r}$, then we can use the following approximation form for $1/|\mathbf{r}_i - \mathbf{r}|$:

$$\frac{Gm_i}{|\mathbf{r}_i - \mathbf{r}|} \approx \frac{Gm_i}{r_i} \left(1 + \frac{\mathbf{r}_i \cdot \mathbf{r}}{r_i^2} + \frac{3(\mathbf{r}_i \cdot \mathbf{r})^2}{2r_i^4} - \frac{1}{2} \frac{r^2}{r_i^2} + \left[\frac{5(\mathbf{r}_i \cdot \mathbf{r})^3}{2r_i^6} - \frac{3\mathbf{r}_i \cdot \mathbf{r}}{2r_i^2} \frac{r^2}{r_i^2} \right] \right) \quad (2.2)$$

The third order terms ([] part in the above equation) can be neglected for the sun but up to third order terms for the moon should be taken into account. Substituting the above equation into the perturbing function, we obtain

$$U_i \approx \frac{Gm_i}{r_i} \left(\frac{3(\mathbf{r}_i \cdot \mathbf{r})^2}{2r_i^4} - \frac{1}{2} \frac{r^2}{r_i^2} + \left[\frac{5(\mathbf{r}_i \cdot \mathbf{r})^3}{2r_i^6} - \frac{3\mathbf{r}_i \cdot \mathbf{r}}{2r_i^2} \frac{r^2}{r_i^2} \right] \right) \quad (2.3)$$

It should be noted that the first term Gm_i/r_i of Eq. (2.2) has been eliminated in Eq. (2.3)

because

$$\nabla \left(\frac{Gm_i}{r_i} \right) = 0 \quad (2.4)$$

Let \mathbf{r}_i be expressed in the satellite coordinate system RSW (Appendix A) as follows:

$$r_i = r_i \begin{bmatrix} p \cos f + q \sin f \\ -p \sin f + q \cos f \\ w \end{bmatrix}_{RSW} \quad (2.5)$$

where the vector (p, q, w) is the perigee vector in the perifocal coordinate system PQW (Appendix A), and f is the true anomaly. Then we obtain

$$\frac{\mathbf{r}_i \cdot \mathbf{r}}{r_i^2} = \frac{r}{r_i} (p \cos f + q \sin f) \quad (2.6)$$

or

$$\frac{\mathbf{r}_i \cdot \mathbf{r}}{r_i^2} = \frac{a}{r_i} \left(p (\cos E - e) + q \sqrt{1 - e^2} \sin E \right) \quad (2.7)$$

where a is the semi-major axis, and e is the eccentricity. The former equation is explicitly expressed in terms of true anomaly, f , while the latter equation is explicitly expressed in terms of eccentric anomaly, E .

Cook³⁾ introduced the approximation in another way,

$$\frac{1}{|\mathbf{r}_i - \mathbf{r}|} \approx \frac{1}{r_i} \left(1 + 3 \frac{r}{r_i} \cos \phi + O \left(\frac{r^2}{r_i^2} \right) \right)^{\frac{1}{3}} \quad (2.8)$$

ϕ is the angle between the radius vector to the satellite and the disturbing body.

$$\cos \phi = \frac{\mathbf{r} \cdot \mathbf{r}_i}{r r_i} = A \cos u + B \sin u \quad (2.9)$$

where u is the argument of latitude which is the sum of the argument of perigee ω and true anomaly f . A and B are calculated from

$$\begin{aligned} A &= \cos(\Omega - \Omega_i) \cos u_i + \cos i_i \sin u_i \sin(\Omega - \Omega_i) \\ B &= \cos i \left[-\sin(\Omega - \Omega_i) \cos u_i + \cos i_i \sin u_i \cos(\Omega - \Omega_i) + \sin i \sin i_i \sin u_i \right] \end{aligned} \quad (2.10)$$

The relationships of A , B , p , and q are as follows

$$\begin{aligned} A \cos u + B \sin u &= p \cos f + q \sin f \\ p &= A \cos \omega + B \sin \omega \\ q &= -A \sin \omega + B \cos \omega \end{aligned} \quad (2.11)$$

In comparison to the complexity of A and B , the calculations of p and q are easier. And the order of

Cook's approximation is first-order whereas the new method is second order. It is obvious the new method is more accurate than conventional method.

Averaging the perturbing function due to the i -th body over one revolution, then we can obtain

$$\begin{aligned}\bar{U}_i &= \frac{1}{P} \int_0^P U_i dt \\ &= \frac{1}{4} \frac{Gm_i}{r_i} \left(\frac{a}{r_i} \right)^3 \left[3p^2 + 3q^2 - 2 + 3e^2 (4p^2 - q^2 - 1) \right] \\ &\quad - \left[\frac{5}{16} \frac{Gm_i}{r_i} \left(\frac{a}{r_i} \right)^3 ep \left\{ 3(5p^2 + 5q^2 - 4) + e^2 (20p^2 - 15q^2 - 9) \right\} \right]\end{aligned}\quad (2.12)$$

Therefore, the rates of change in the orbital elements can be calculated. The equations of the results are written in Appendix C.

These equations give very good accuracy of the satellite orbit for long-term computations although there are fewer terms of calculation than in Cook's method. The simulation results of comparisons between this new method and Cook's method will be shown in section 4.

3. Atmospheric Drag

The effect of the atmospheric drag is the most important perturbing force in low earth orbit because it is the only drag force which causes reentry. The functions for long-term calculation of the atmospheric drag were developed by King-Hele⁴⁾ which work well but are complicated. In this section, simplified method for long-term computation of the effects of atmospheric drag considering the rotation of the Earth is derived.

A specific acceleration is shown by

$$\mathbf{a}_{drag} = -\frac{1}{2} \frac{c_D A}{m} \rho v_{rel} \mathbf{v}_{rel} \quad (3.1)$$

where c_D is the drag coefficient which is a dimensionless value which reflects the satellite's susceptibility to drag forces. The drag coefficient for satellites in the upper atmosphere is often considered to be approximately $c_D \sim 2.0$. Spheres have $c_D \sim 1.0$. The drag coefficient is configuration-specific and is seldom approximated to more than three significant digits. The atmospheric density, ρ , indicates how dense the atmosphere is at a given altitude and is perhaps the most difficult parameter to determine. Another difficult parameter to estimate is the cross-sectional area, A , defined to be the area that is normal to the satellite's velocity vector. For a tumbling reentry vehicle, such as Skylab in 1980, it is nearly impossible to know the attitude accurately, so A is inherently uncertain. We also need the satellite's mass, m , along with the relative-velocity vector.

For some satellites, we cannot assume that the mass is constant. Recognize the v_{rel} is not the velocity vector typically found in the state vector. This velocity vector is relative to the atmosphere. Actually, the Earth's atmosphere has a mean motion due to the Earth's rotation, and the local winds are superimposed on this mean motion. Notice also that the force of drag is opposite to the velocity vector at all times. This is the primary use for the *NTW* coordinate system. In this system, the primary axis (N) lies in the orbital plane, normal to the velocity vector. The T axis is tangential to the orbit, and the W axis is normal to the orbital plane as in the *RSW* system. For a non-spherical satellite, we must also consider companion aerodynamic forces such as lift and drag forces.

We usually call $m/(c_D A)$ the ballistic coefficient, BC , it represents another measure of the satellite's susceptibility to drag effects. With this definition, a low BC means that drag will affect the satellite significantly and vice versa. These quantities have many definitions, so it's very important to understand which one is being used.

The velocity vector relative to the rotating atmosphere is given by

$$\mathbf{v}_{rel} = \frac{d\mathbf{r}}{dt} - \boldsymbol{\omega}_{Earth} \times \mathbf{r} \quad (3.2)$$

Escobal²⁶⁾ gives a more general expression including wind variations, which requires the wind's speed, v_w , and azimuth, β_w , and the satellite's right ascension and declination. But many applications do not use this expression because the additional information is usually not available. Instead, the satellite's specific orientation and shape are determined to help determine the satellite's effective cross-sectional area. Now, we will derive an expression for the velocity vector relative to the rotating atmosphere. Consider the RSW coordinate system (See Appendix A), then the vectors

$d\mathbf{r}/dt$, the Earth's rotational velocity $\boldsymbol{\omega}_{Earth}$, and the distance from the earth \mathbf{r} in Eq. (3.2) can be expressed by

$$\frac{d\mathbf{r}}{dt} = \begin{bmatrix} \dot{r} \\ r\dot{f} \\ 0 \end{bmatrix}_{RSW}, \quad \boldsymbol{\omega}_{Earth} = [R]^T \begin{bmatrix} 0 \\ 0 \\ \omega_{Earth} \end{bmatrix} = \begin{bmatrix} \omega_{Earth} R_{31} \\ \omega_{Earth} R_{32} \\ \omega_{Earth} R_{33} \end{bmatrix}_{RSW} \quad \text{and} \quad \mathbf{r} = \begin{bmatrix} r \\ 0 \\ 0 \end{bmatrix}_{RSW} \quad (3.3)$$

respectively. The Earth's rotational velocity $\boldsymbol{\omega}_{Earth}$ is often assumed to be constant, and indeed it seemed to be so for many years, given the limits of measuring devices. Most applications use the adopted constant value for the Earth's rotation:

$$\omega_{Earth} = 7.29115 \times 10^{-5} \pm 1.5 \times 10^{-12} [\text{rad} / \text{s}] \quad (3.4)$$

Submitting the above vectors into Eq. (3.1), we obtain the expression of the velocity vector relative to the rotating atmosphere in the RSW coordinate system.

$$\mathbf{v}_{rel} = \begin{bmatrix} \dot{r} \\ r\dot{f} - \omega_{Earth} r R_{33} \\ \omega_{Earth} r R_{32} \end{bmatrix}_{RSW} \quad (3.5)$$

For convenience, the equations shown below may be useful

$$\dot{r} = \frac{h}{p} e \sin f, \quad r\dot{f} = \frac{h}{r} = \frac{h}{p} (1 + e \cos f), \quad R_{33} = \cos i, \quad R_{32} = \cos u \sin i \quad (3.6)$$

where p is the semi-latus rectum and h is the specific angular momentum, f is the true anomaly, and u is the sum of the argument perigee, ω , and the true anomaly.

A general method to obtain the first-order solution according to King-Hele⁴⁾ will be described here. This method uses the eccentric anomaly, E , as independent variable, and uses a power series of $e \cos E$ valid for $e < 0.2$. However, we use the expressions derived by Blizer¹¹⁾. Since the geocentric latitude, ϕ , is given by

$$\sin \phi = \sin u \sin i \quad (3.7)$$

the magnitude of $\omega_{Earth} \times r$ can be expressed in terms of geocentric latitude as

$$|\omega_{Earth} \times \mathbf{r}| = \omega_{Earth} r \cos \phi \quad (3.8)$$

If γ denotes the angle between $d\mathbf{r}/dt$ ($= \mathbf{v}$) and $\omega_{Earth} \times \mathbf{r}$, the magnitude of the velocity vector relative to the rotating atmosphere can be expressed as

$$v_{rel}^2 = v^2 - 2v\omega_{Earth} r \cos \phi \cos \gamma + \omega_{Earth}^2 r^2 \cos^2 \phi \quad (3.9)$$

where v denotes the magnitude of dr/dt , giving

$$v^2 = \dot{r}^2 + (r\dot{f})^2 = \frac{h^2}{p^2} (1 + e^2 + 2e \cos f) \quad (3.10)$$

From spherical trigonometry, we have

$$\cos \phi \cos \gamma = \cos i$$

Then Eq. (3.9) becomes

$$\begin{aligned} v_{rel}^2 &= v^2 - 2v\omega_{Earth} r \cos i + \omega_{Earth}^2 r^2 \cos^2 \phi \\ &= v^2 \left(1 - \frac{\omega_{Earth} r}{v} \cos i \right)^2 + \omega_{Earth}^2 r^2 (\cos^2 \phi - \cos^2 i) \end{aligned} \quad (3.11)$$

As the effect of atmospheric rotation on drag is small and ω_{Earth} may vary unpredictably by $\pm 5\%$,

we should seek approximations in Eq. (3.11). The $\omega_{Earth}^2 r^2$ terms can be neglected, since

$\omega_{Earth}^2 r^2 < 0.005v_{rel}^2$, and in the $\omega_{Earth}^2 r/v$ term we may take $r/v = r_p/v_p$, where suffix p

denotes values at perigee. As the main effects of drag at heights not more than $2H$ above perigee, where r/v does not differ from r_p/v_p by more than 4% if $H/r_p < 0.01$, and the effects are weighted towards perigee, the error in this last approximation will be less than 2% . Thus, Eq. (3.11) may be rewritten as

$$v_{rel} = v \left(1 - \frac{\omega_{Earth} r_p}{v_p} \cos i \right) \quad (3.12)$$

Although the expression is really an approximation, it has been written as an equality, because an error of 2% in the ω_{Earth} term leads to an error of only 0.1% and this is also considerably smaller than the likely error due to lack of knowledge of ω_{Earth} . Since r_p , v_p and i often change little during a satellite's life, it may be possible to use the initial values of all three parameters in Eq. (3.12). On substituting Eq. (3.12) into Eq. (3.1), the magnitude of the specific disturbing acceleration due to drag may be rewritten as

$$a_{drag} = -\frac{1}{2} \rho v^2 \delta \quad (3.13)$$

parallel, but in the opposite sense, to \mathbf{v}_{rel} , the velocity of the satellite relative to the ambient air. The parameter δ is given by

$$\delta = \frac{c_D A}{m} Q, \quad Q = \left(1 - \frac{\omega_{Earth} r_p}{v_p} \cos i \right)^2 \quad (3.14)$$

3.1 Changes in a and e due to drag

The sine of the angle between \mathbf{v}_{rel} and \mathbf{v} never exceeds $\omega_{Earth}r/v$ or 0.07 for a near-Earth satellite. Therefore, its cosine always exceeds 0.997 and can be taken as unity. Thus the specific acceleration due to drag tangential to the orbit is given by

$$F_t = -\frac{1}{2}\rho v^2 \delta \quad (3.15)$$

The specific acceleration normal to the orbit in the orbital plane can be ignored until we take into account the effects of atmospheric rotation on the orientation of the orbital plane. With these two simplifications, we can now write down the equations for the rates of change of a and e , by substituting Eq. (3.15) into Eqs. (6.13-14).

$$\frac{da}{dt} = -\frac{\rho v^3 \delta}{n^2 a} \quad (3.16)$$

$$\frac{de}{dt} = -(e + \cos f) \rho v \delta \quad (3.17)$$

It is more convenient to work in terms of the eccentric anomaly E than the true anomaly f .

$$ndt = (1 - e \cos E) dE \quad \text{and} \quad e + \cos f = \frac{\cos E - e}{1 - e \cos E} \quad (3.18)$$

Using Eq. (3.18), then Eqs. (3.16-17) may be written

$$\frac{da}{dE} = -\frac{\rho v^3 \delta}{n^3 a} (1 - e \cos E) \quad (3.19)$$

$$\frac{de}{dE} = -\frac{1 - e^2}{n} \rho v \delta \cos E \quad (3.20)$$

The velocity v can be expressed in terms of the eccentric anomaly E as

$$v = na \sqrt{\frac{1 + e \cos E}{1 - e \cos E}} \quad (3.21)$$

Substituting Eq. (3.21) into Eqs. (3.19-20), we obtain

$$\frac{da}{dE} = -a^2 \rho \delta \frac{(1 + e \cos E)^{3/2}}{(1 - e \cos E)^{1/2}} \quad (3.22)$$

$$\frac{de}{dE} = -a \rho \delta \left(\frac{1 + e \cos E}{1 - e \cos E} \right)^{1/2} (1 - e^2) \cos E \quad (3.23)$$

The change of a and e during a revolution, Δa_{rev} and Δe_{rev} , are obtained by integrating Eqs. (3.22-23) from $E = 0$ to $E = 2\pi$. Thus,

$$\Delta a_{rev} = -a^2 \delta \int_0^{2\pi} \frac{(1 + e \cos E)^{3/2}}{(1 - e \cos E)^{1/2}} \rho dE \quad (3.24)$$

$$\Delta e_{rev} = -a\delta \int_0^{2\pi} \left(\frac{1+e \cos E}{1-e \cos E} \right)^{1/2} (1-e^2) \rho \cos E dE \quad (3.25)$$

In this method, we take the simplest model for air density, assuming that the density ρ depends solely on the distance r from the Earth's center and varies exponentially with r , with the density scale height H being constant. Thus we may write

$$\rho = \rho_p \exp\left(-\frac{r-r_p}{H}\right) \quad (3.26)$$

where ρ is the density at the initial perigee point at distance r_p from the Earth's center. Recalling that:

$$r = a(1-e \cos E) \quad \text{and} \quad r_p = a(1-e) \quad (3.27)$$

and assuming that the variables in brackets in Eq. (3.26) change little over a revolution, we can rewrite Eq. (3.26) as

$$\rho = \rho_p \exp[c \cos E - c] \quad (3.28)$$

where $c = ae/H$.

Substituting Eq. (3.28) into Eqs. (3.24-25), we obtain

$$\Delta a_{rev} = -a^2 \rho_p \delta \exp[-c] \int_0^{2\pi} \frac{(1+e \cos E)^{3/2}}{(1-e \cos E)^{1/2}} \exp[c \cos E] dE \quad (3.29)$$

$$\Delta e_{rev} = -a \rho_p \delta \exp[-c] \int_0^{2\pi} \left(\frac{1+e \cos E}{1-e \cos E} \right)^{1/2} (1-e^2) \cos E \exp[c \cos E] dE$$

For $e < 0.2$, expanding the integrals as power series in e , the Eqs. (3.29) become

$$\begin{aligned} \Delta a_{rev} &= -a^2 \rho_p \delta \exp[-c] \int_0^{2\pi} \exp[c \cos E] \\ &\quad \left(1 + 2e \cos E + \frac{3e^2}{4} (1 + \cos 2E) + \frac{e^3}{4} (3 \cos E + \cos 3E) + O(e^4) \right) dE \\ \Delta e_{rev} &= -a \rho_p \delta \exp[-c] \int_0^{2\pi} \exp[c \cos E] \left(\cos E + \frac{e}{2} (1 + \cos 2E) \right. \\ &\quad \left. - \frac{e^2}{8} (5 \cos E - \cos 3E) - \frac{e^3}{16} (5 + 4 \cos 2E - \cos 4E) + O(e^4) \right) dE \end{aligned} \quad (3.30)$$

Using the integral representation of the modified Bessel function of the first kind, I_j , given by

$$I_j(c) = \frac{1}{2\pi} \int_0^{2\pi} \cos jE \exp[c \cos E] dE \quad (3.31)$$

then the terms in Eqs. (3.30) can be integrated individually. The results of the analytical solution are shown in Appendix D.

3.2 Changes in i and Ω due to drag

The Gaussian planetary equations, Eqs. (B.2), show that the only orbital elements directly

affected by F_w are the inclination i and the right ascension of the node Ω ; but the change in Ω is partially transmitted to the argument of perigee ω , as Eqs. (B.2) shows. This ‘knock-on effect’ is usually negligible. The magnitude of the specific acceleration due to drag given by Eq. (3.13) is parallel but in the opposite sense, to \mathbf{v}_{rel} , the velocity of the satellite relative to the ambient air. Since the orbital velocity \mathbf{v} should be in the orbital plane and \mathbf{v}_{rel} makes an angle γ with the orbital plane, the component of \mathbf{v}_{rel} perpendicular to the orbital plane is

$$(\mathbf{v}_{rel})_w = \omega_{Earth} r \cos \phi \sin \gamma \quad (3.32)$$

On applying the cosine formula, we may rewrite Eq. (3.32) as

$$(\mathbf{v}_{rel})_w = \omega_{Earth} r \sin i \cos u \quad (3.33)$$

Hence the specific acceleration due to drag in the T axis is

$$F_t = -\frac{1}{2} \rho v^2 \delta \frac{\omega_{Earth} r \sin i \cos u}{v_{rel}} = -\frac{1}{2} \rho v \frac{\delta}{\sqrt{Q}} \omega_{Earth} r \sin i \cos u \quad (3.34)$$

Substituting Eq. (3.34) into Eqs. (B.2), then we obtain the rate of the changes in i and Ω as

$$\frac{di}{dt} = -\frac{\rho v \delta \omega_{Earth} r^2}{2na^2 \sqrt{1-e^2} \sqrt{Q}} \sin i \cos^2 u \quad (3.35)$$

$$\frac{d\Omega}{dt} = -\frac{\rho v \delta \omega_{Earth} r^2}{2na^2 \sqrt{1-e^2} \sqrt{Q}} \sin u \cos u \quad (3.36)$$

Eliminating dt and v by use of Eqs. (3.18) and (3.21), then we obtain

$$\frac{di}{dE} = -\frac{\rho \delta \omega_{Earth} \sqrt{(1-e \cos E)(1+\cos E)}}{2na \sqrt{1-e^2} \sqrt{Q}} r^2 \sin i \cos^2(\omega + f) \quad (3.37)$$

$$\frac{d\Omega}{dt} = -\frac{\rho \delta \omega_{Earth} \sqrt{(1-e \cos E)(1+e \cos E)}}{2a \sqrt{1-e^2} \sqrt{Q}} r^2 \sin(\omega + f) \cos(\omega + f) \quad (3.38)$$

r , $\sin f$ and $\cos f$ may be expressed in terms of the eccentric anomaly E as

$$r = a(1 - e \cos E), \quad \sin f = \frac{\sqrt{1-e^2} \sin E}{1 - e \cos E}, \quad \text{and} \quad \cos f = \frac{\cos E - e}{1 - e \cos E} \quad (3.39)$$

Utilizing the above relations and expanding in power of e , we may rewrite Eqs. (3.37-38) as

$$\frac{di}{dt} = -\frac{a \rho \delta \omega_{Earth}}{2n \sqrt{Q}} \sin i \left(\cos^2(\omega + E) - 2e \cos \omega \cos(\omega + E) + O(e^2) \right) \quad (3.40)$$

$$\frac{d\Omega}{dt} = -\frac{a \rho \delta \omega_{Earth}}{2n \sqrt{Q}} \left(\sin(\omega + E) \cos(\omega + E) - e \sin(2\omega + E) + O(e^2) \right) \quad (3.41)$$

We assume an exponential variation of air density with height as in Eq. (3.26). Substituting for ρ from Eq. (3.28), and integrating, Eqs. (3.37-38) gives the change in i and Ω over a revolution:

$$\begin{aligned} \Delta i_{rev} = & -\frac{a \rho_p \delta \omega_{Earth}}{2n \sqrt{Q}} \frac{\sin i}{2} \exp[-c] \int_0^{2\pi} \exp(c \cos E) (1 - 2e \cos E \\ & + (\cos 2E - 2e \cos E) \cos 2\omega - (\sin 2E - 2e \sin E) \sin 2\omega + O(e^2)) dE \end{aligned} \quad (3.42)$$

$$\begin{aligned} \Delta\Omega_{rev} = & -\frac{a\rho_p \delta\omega_{Earth}}{2n\sqrt{Q}} \frac{1}{2} \exp[-c] \int_0^{2\pi} \exp[c \cos E] \left((\sin eE - 2e \sin E) \cos 2\omega \right. \\ & \left. + (\cos 2E - 2e \cos E) \sin 2\omega + O(e^2) \right) dE \end{aligned} \quad (3.43)$$

Since

$$\int_0^{2\pi} \sin jE \exp[c \cos E] dE = 0 \quad (3.44)$$

for any integer j terms in $\sin E$ and $\sin 2E$ within the integrals in Eqs. (3.42-3.43) can be dropped. Utilizing the integral representation of I_j given in Eq. (3.31), then we may rewrite Eqs. (3.42-3.43). The equation of the results are written in Appendix D.

3.3 Changes in ω and M_0 due to drag

Applying the same methods described in the previous sections to Eqs. (B.2), then we find

$$\int_0^{2\pi} \left(\frac{d\omega}{dE} + \frac{d\Omega}{dE} \cos i \right) dE = 0 \quad \text{and} \quad \int_0^{2\pi} \frac{dM_0}{dE} dE = 0 \quad (3.45)$$

since the integrals have only $\sin(jE)$ that can be dropped by Eq. (3.44). Therefore, we obtain

$$\Delta\omega_{rev} = -\Delta\Omega_{rev} \cos i \quad \text{and} \quad \Delta M_0 = 0 \quad (3.46)$$

Other perturbing functions due to the solar radiation pressure and zonal harmonics are shown in Appendix E and F.

4. Simulations

We compared the present method with Cook's method and the actual orbital evolution of a couple of objects in low Earth orbit and in geostationary transfer orbit.

Figures 4-1 and **4-2** compare the changes in orbital elements in low Earth orbit. The space object of this test case is Explorer 9 (1961-004A) which was launched on February 16th, 1961, by the United States. As the figures show, Cook's method and the new method provide similar orbital evolutions. Compared with historical evolution, the reentry dates are different because our propagator uses simple exponential model as the atmospheric density model. If we introduce a more accurate atmospheric density model, it would get closer to the actual orbit. The orbit of Explorer 9 was circular and eccentricity was small (approximately 0.1). Orbital evolutions are not different when using new method on the conventional method in such a case because both expressions become similar when the eccentricity has small value.

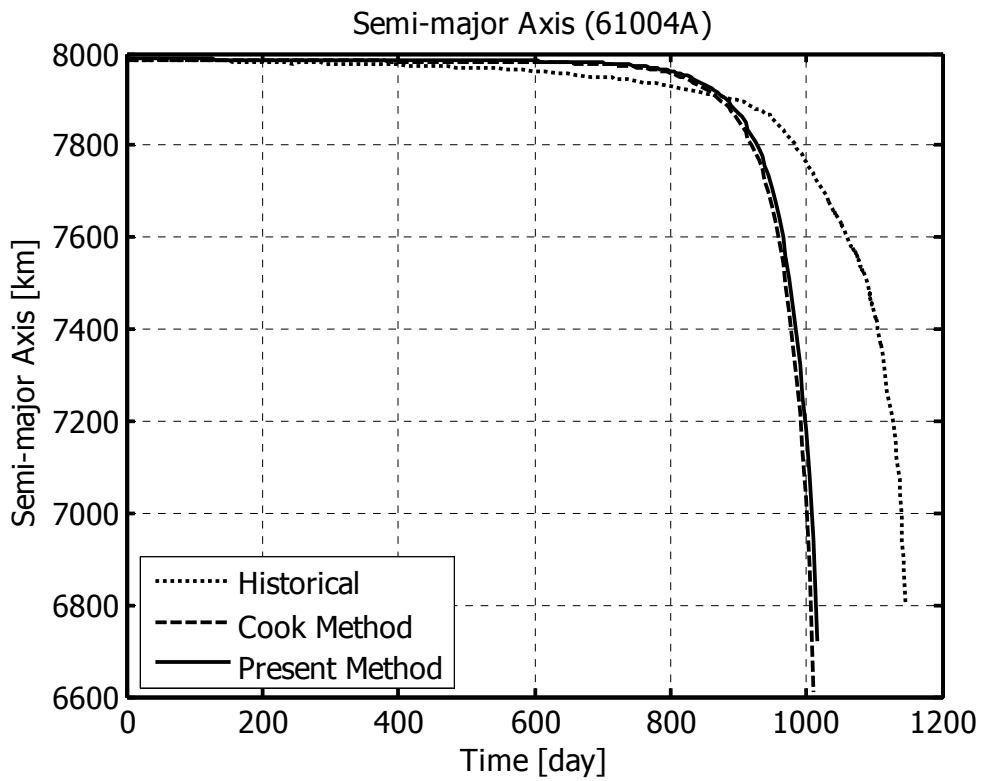


Fig. 4-1 Semi-major Axis (1961-004A).

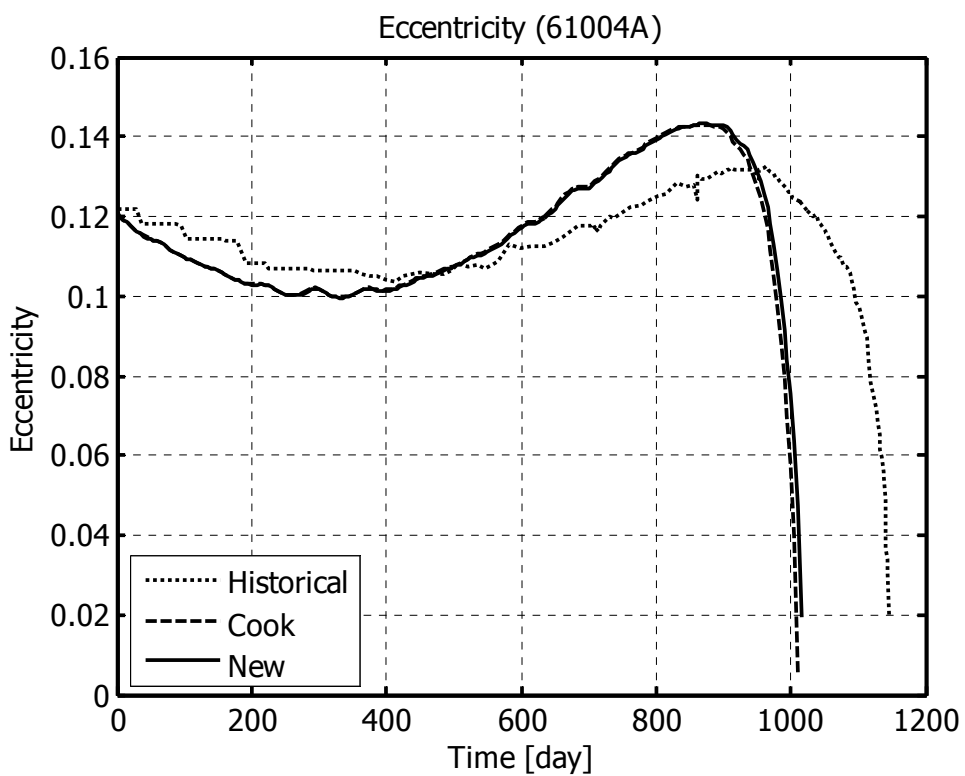


Fig. 4-2 Eccentricity (1961-004A).

Figures 4-3 and 4-4 show results of the comparison in Geostationary Transfer Orbit (GTO). The space object is the rocket body which transferred the satellite Cosmos 41. The semi-major axes do not change between using Cook's method and the new method because the short-periodic terms are neglected. In terms of the eccentricity, the new method works well compared to Cook's method. The space object dropped to the Earth because the eccentricity increased too much. The reason why Cook's method does not calculate the eccentricity correctly is that the perturbing equations assume that the eccentricity is small value because he assumes

$$\frac{a}{r_i} \ll 1 \quad (4.1)$$

therefore, the terms corresponding $(a/r_i)^2$ in Eqs. (C.1) are neglected in Cook's method but not in the new method. Additionally, the time of computation of Cook's method is larger compared with the new method whereas the accuracy is not as good. It is obvious that new method is superior to the conventional method.

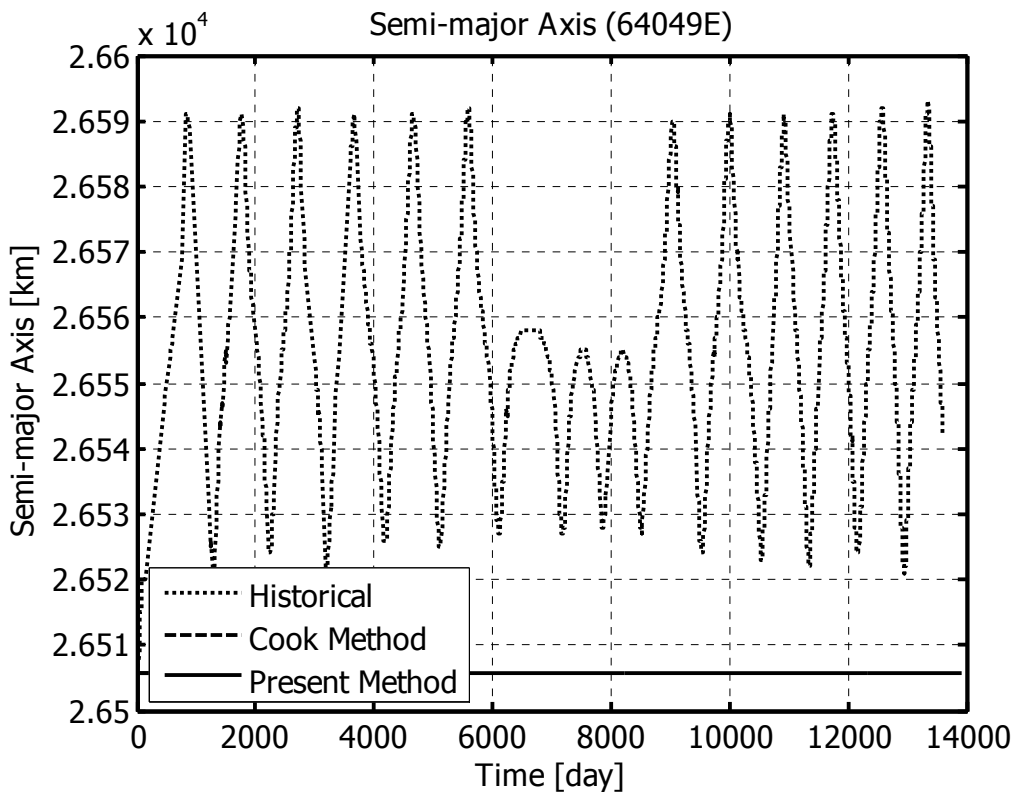


Fig. 4-3 Semi-major Axis (1964-049E).

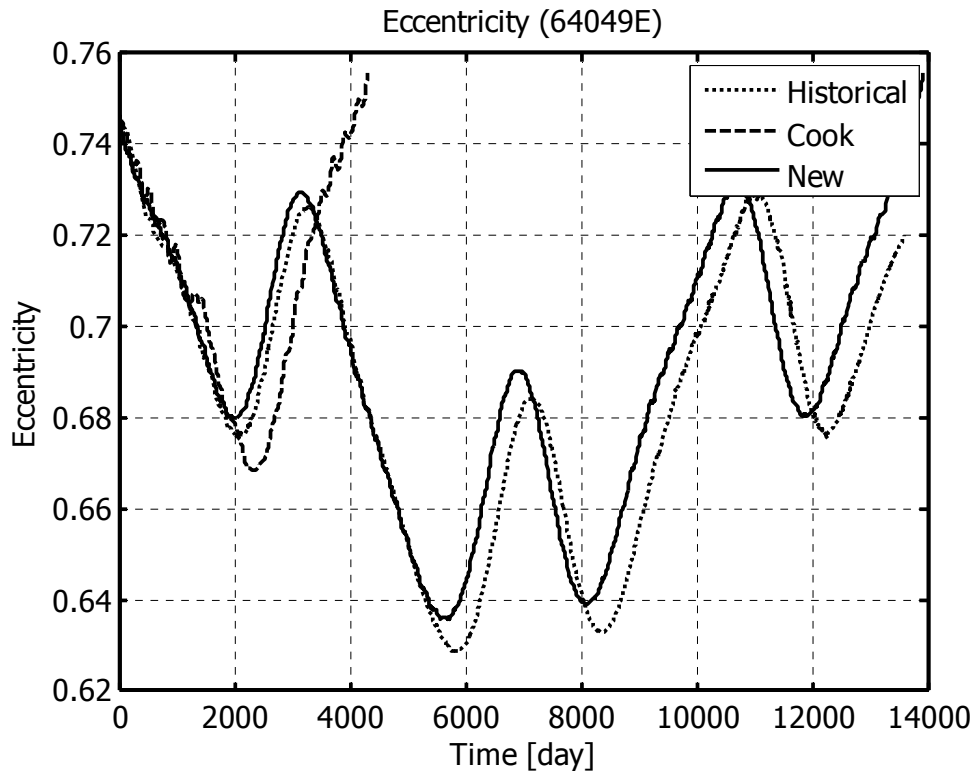


Fig. 4-4 Eccentricity (1964-049A).

5. Conclusion

A new analytical model has been established for computing the long-term orbital evolutions of space objects using a new approximation technique of perturbing functions. A few simulations of the model have been presented to demonstrate the long-term prediction of orbits, and the results are found to be useful for long-term computation in any elliptic orbit, in fact better than conventional methods. This new method was invented for investigating the evolution of space debris in the future. Actually the new method has been built in the orbital debris environment evolutionary models at Kyushu University and Johnson Space Center, National Aeronautics and Space Administration (NASA). The model can be a practical tool for predicting or designing orbits of space objects.

References

- (1) Vallado, D. A., Fundamentals of Astrodynamics and Applications, Second Edition, Microcosm Press and Kluwer academic, US, 2001.
- (2) Chobotov, V. A., Editor, Orbital Mechanics Second Edition, AIAA Education Series, Virginia, 1996.
- (3) Cook, G. E., Luni-Solar Perturbations of the Orbit of an Earth Satellite, The Geophysical Journal, Vol. 6, No. 3, pp. 271-291, 1962.
- (4) King-Hele, D., Satellite Orbit in an Atmosphere, Blackie and Son, London, pp. 44-46, 1975.
- (5) Vinti, J. P., Orbital and Celestial Mechanics, Progress in Astronautical and Aeronautics,

- Vol.177, Chap. 17, pp.193- 206,American Institute of Aeronautics and Astronautics, Reston, VA, 1998.
- (6) Hanada, T. and Yasaka, T., GEODEEM 3.0: Updated Kyushu University GEO Model, Proceedings of the 24th International Symposium on Space Technology and Science, JSASS, Tokyo, pp.946-951, 2004.
 - (7) Meeus, J., *Astronomical Algorithms*, Second Edition, Willmann-Bell Inc., US, 1998.
 - (8) van der Ha, J. C., Long-Term Evolution of Near-Geostationary Orbits, *Journal of Guidance, Control, and Dynamics*, Vol. 9, Issue 3 , pp. 363-370, May 1986.
 - (9) Montenbruck, O. and Gill, E., *Satellite Orbits - Models, Methods, and Applications*; Springer-Verlag, Heidelberg, 2000.
 - (10) Baker, R. M. L. and Makemson, M. W., *An Introduction to Astrodynamics*, Akademic Press, New York, 1960.
 - (11) Blitzer, L., *Amer. J. Physics*, Vol. 27, No. 634, 1959.
 - (12) Brown, E. W. and Shook, C. A., *Planetary Theory*, Cambridge University Press, 1933.
 - (13) Geyling, F. T., *J. Franklin Inst.*, Vol. 269, No. 375, 1960.
 - (14) Hynek, J. A. (Ed.), *Astrophysics*, McGraw Hill Book Co., Inc., New York, 1951.
 - (15) King-Hele, D. G., *Proc. Roy. Soc., A*, Vol. 247, No. 49, 1958.
 - (16) King-Hele, D. G., *Geophys. J.*, Vol. 4, No. 3, 1961.
 - (17) Kozai, Y., *Smithsonian Institution Astrophysical Observatory*, Special Report No. 22, 1959.
 - (18) Moe, M. M., *A. R. S. Journal*, Vol. 30, No. 485, 1960.
 - (19) Musen, P., *Space Research: Proceedings of the first international space science symposium*, Nice, North Holland Pub. Co., Amsterdam, pp. 434-, 1960.
 - (20) Musen, P., *J. Geophys. Res.*, Vol. 65, No. 1931, 1960b.
 - (21) Musen, P., Bryant, R. and Bailie, A., *Science*, Vol. 131, No. 935, 1960.
 - (22) Smart, W. M., *Celestial Mechanics*, Longmans, Green and Co., London, 1953.
 - (23) Spitzer, L., *J. Brit. Interplanet. Soc.*, Vol. 9, No. 131, 1950.
 - (24) Tisserand, F., *Traite de Mechanique Celeste*, Vol. 1, Paris, 1889.
 - (25) Upton, E., Bailie, A. and Musen, P., *Science*, Vol. 130, No. 1710, 1959.
 - (26) Escobal, P. R., *Methods of orbit determination*, Robert E. Krieger, NewYork,1976.

Appendix A. Coordinate Systems

Figure A-1 shows the Satellite Local Coordinate System which applies to studies of relative motion. R is defined as always pointing from the Earth's center to the satellite and W is fixed along the direction normal to the orbital plane in direction of angular momentum. S is perpendicular to R and W axes.

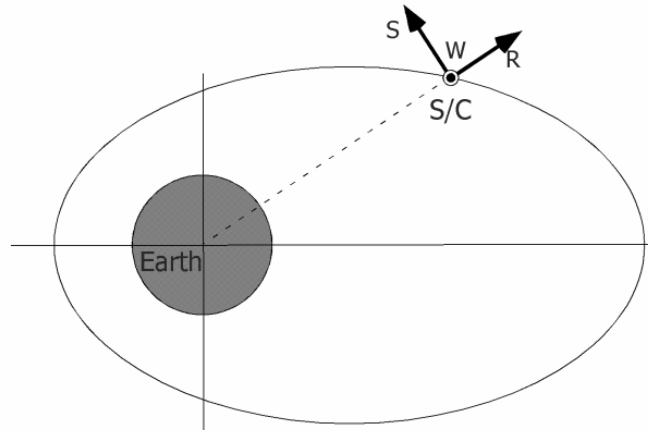


Fig. A-1 Satellite Coordinate System (RSW).

Figure A-2 shows the Perifocal Coordinate System which is a convenient for processing satellite observations. The origin is at the center of the Earth, and the fundamental plane is the satellite orbit. P points towards perigee, and Q is 90 degrees from the P axis in the direction of satellite motion. W is normal to the orbit.

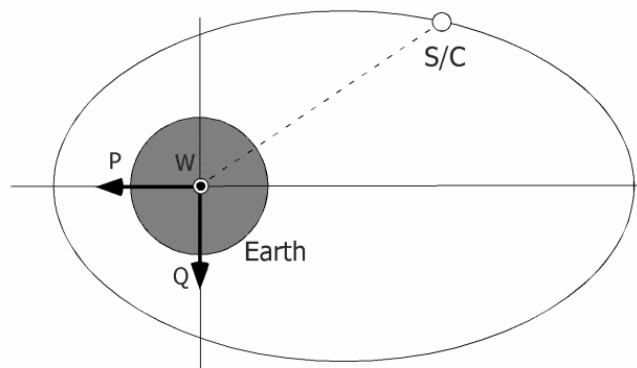


Fig. A-2 Perifocal Coordinate System (PQW).

Appendix B. Planetary Equations

B. 1 Lagrange planetary equations

According to Vallado¹⁾, Lagrange planetary equations is given by

$$\frac{da}{dt} = \frac{2}{na} \frac{\partial R}{\partial M}$$

$$\begin{aligned}
\frac{de}{dt} &= \frac{1-e^2}{na^2e} \frac{\partial R}{\partial M} - \frac{\sqrt{1-e^2}}{na^2e} \frac{\partial R}{\partial \omega} \\
\frac{di}{dt} &= \frac{1}{na^2\sqrt{1-e^2} \sin i} \left(\cos i \frac{\partial R}{\partial \omega} - \frac{\partial R}{\partial \Omega} \right) \\
\frac{d\Omega}{dt} &= \frac{1}{na^2\sqrt{1-e^2} \sin i} \frac{\partial R}{\partial i} \\
\frac{d\omega}{dt} + \frac{d\Omega}{dt} \cos i &= \frac{\sqrt{1-e^2}}{na^2e} \frac{\partial R}{\partial e} \\
\frac{dM_0}{dt} &= -\frac{1-e^2}{na^2e} \frac{\partial R}{\partial a} \\
&= -\frac{2}{na} \frac{\partial R}{\partial a} - \sqrt{1-e^2} \left(\frac{d\omega}{dt} + \frac{d\Omega}{dt} \cos i \right)
\end{aligned} \tag{B.1}$$

B.2 Gaussian planetary equations (RSW coordinate system)

According to Vallado¹⁾, the Gaussian form of the planetary equations in the RSW coordinate system is given by

$$\begin{aligned}
\frac{da}{dt} &= \frac{2}{n\sqrt{1-e^2}} \left[F_r e \sin f + F_s (1+e \cos f) \right] \\
\frac{de}{dt} &= \frac{\sqrt{1-e^2}}{na} \left[F_r \sin f + F_s \left(\cos f + \frac{e + \cos f}{1+e \cos f} \right) \right] \\
\frac{di}{dt} &= F_w \frac{r \cos u}{na^2\sqrt{1-e^2}} \\
\frac{d\Omega}{dt} &= F_w \frac{r \sin u}{na^2\sqrt{1-e^2} \sin i} \\
\frac{d\omega}{dt} + \frac{d\Omega}{dt} \cos i &= -\frac{\sqrt{1-e^2}}{nae} \left[F_r \cos f - F_s \left(\sin f + \frac{\sin f}{1+e \cos f} \right) \right] \\
\frac{dM}{dt} + \sqrt{1-e^2} \left(\frac{d\omega}{dt} + \frac{d\Omega}{dt} \cos i \right) &= n - F_r \frac{2r}{na^2}
\end{aligned} \tag{B.2}$$

where (F_r, F_s, F_w) are the components of the force vector.

Appendix C. Perturbation Due to the I -th Body

$$\dot{a} = 0$$

$$\begin{aligned} \dot{e} &= -\frac{15\sqrt{1-e^2}}{2} \frac{Gm_i}{na} \frac{a}{r_i^2} \frac{a}{r_i} (epq) \\ &+ \left[\frac{15\sqrt{1-e^2}}{16} \frac{Gm_i}{na} \frac{Gm_i}{r_i^2} \left(\frac{a}{r_i}\right)^2 q (5p^2 + 5q^2 - 4 + e^2(30p^2 - 5q^2 - 3)) \right] \\ \\ \dot{i} &= \frac{3}{2} \frac{w}{na\sqrt{1-e^2}} \frac{Gm_i}{r_i^2} \frac{a}{r_i} \left((1+4e^2)p \cos \omega - (1-e^2)q \sin \omega \right) \\ &- \left[\frac{15}{16} \frac{ew}{na\sqrt{1-e^2}} \frac{Gm_i}{r_i^2} \left(\frac{a}{r_i}\right)^2 \left((15p^2 + 5q^2 - 4 + e^2(20p^2 - 5q^2 - 3)) \right. \right. \\ &\left. \left. \times \cos \omega - 10(1-e^2)pq \sin \omega \right) \right] \\ \\ \dot{\Omega} &= \frac{3}{2} \frac{w \csc i}{na\sqrt{1-e^2}} \frac{Gm_i}{r_i^2} \frac{a}{r_i} \left((1+4e^2)p \sin \omega + (1-e^2)q \cos \omega \right) \\ &- \left[\frac{15}{16} \frac{ew \csc i}{na\sqrt{1-e^2}} \frac{Gm_i}{r_i^2} \left(\frac{a}{r_i}\right)^2 \left((15p^2 + 5q^2 - 4 + e^2(20p^2 - 5q^2 - 3)) \right. \right. \\ &\left. \left. \times \sin \omega + 10(1-e^2)pq \cos \omega \right) \right] \\ \\ \dot{\omega} + \dot{\Omega} \cos i &= \frac{3\sqrt{1-e^2}}{2} \frac{Gm_i}{na} \frac{a}{r_i^2} (4p^2 - q^2 - 1) \\ &- \left[\frac{15\sqrt{1-e^2}}{16} \frac{Gm_i}{na} \frac{Gm_i}{r_i^2} \left(\frac{a}{r_i}\right)^2 p (5p^2 + 5q^2 - 4 + e^2(20p^2 - 5q^2 - 9)) \right] \\ \\ \dot{M}_0 + \sqrt{1-e^2} (\dot{\omega} + \dot{\Omega} \cos i) &= -\frac{1}{na} \frac{Gm_i}{r_i^2} \frac{a}{r_i} (3p^2 + 3q^2 - 2 + 3e^2(4p^2 - q^2 - 1)) \\ &+ \left[\frac{15}{8} \frac{1}{na} \frac{Gm_i}{r_i^2} \left(\frac{a}{r_i}\right)^2 ep (3(5p^2 + 5q^2 - 4) + e^2(20p^2 - 15q^2 - 9)) \right] \end{aligned} \tag{C.1}$$

Appendix D. Perturbation Due to Atmospheric Drag

$$\begin{aligned}
\Delta a_{rev} &= -2\pi a^2 \rho_p \delta \left(I_0 + 2eI_1 + \frac{3}{4}e^2(I_0 + I_2) + \frac{e^3}{4}(3I_1 + I_3) + O(e^4) \right) \exp[-c] \\
\Delta e_{rev} &= -2\pi a \rho_p \delta \left(I_1 + \frac{e}{2}(I_0 + I_2) - \frac{e^2}{8}(5I_1 - I_3) - \frac{e^3}{16}(5I_0 + 4I_2 - I_4) + O(e^4) \right) \exp[-c] \\
\Delta i_{rev} &= -\frac{\pi a \rho_p \delta \omega_{Earth}}{2n\sqrt{\Omega}} \sin i (I_0 - 2eI_1 + (I_2 - 2eI_1) \cos 2\omega + O(e^2)) \exp[-c] \\
\Delta \Omega_{rev} &= -\frac{\pi a \rho_p \delta \omega_{Earth}}{2n\sqrt{\Omega}} ((I_2 - 2eI_1) \sin 2\omega + O(e^2)) \exp[-c] \\
\Delta \omega_{rev} &= -\Delta \Omega_{rev} \cos i \\
\Delta M_0 &= 0
\end{aligned} \tag{D.1}$$

Appendix E. Perturbation Due to Solar Radiation Pressure

Most satellites including geosynchronous satellites experience occasional eclipses. The solar radiation pressure is not a conservative force so we use Gaussian Planetary Equations to obtain a first-order solution. According to Vinti⁵⁾, the rate of changes of the orbital elements become

$$\begin{aligned}
\dot{a} &= 0 \\
\dot{e} &= -F_s \frac{1}{r_i^2} \frac{3}{2} \frac{q\sqrt{1-e^2}}{na} \\
\dot{i} &= F_s \frac{1}{r_i^2} \frac{3}{2} \frac{ew \cos \omega}{na\sqrt{1-e^2}} \\
\dot{\Omega} &= F_s \frac{1}{r_i^2} \frac{3}{2} \frac{ew \sin \omega}{na\sqrt{1-e^2} \sin i} \\
\dot{\omega} + \dot{\Omega} \cos i &= F_s \frac{1}{r_i^2} \frac{3}{2} \frac{p\sqrt{1-e^2}}{nae} \\
\dot{M}_0 + \sqrt{1-e^2} (\dot{\omega} + \dot{\Omega} \cos i) &= -F_s \frac{1}{r_i^2} \frac{3ep}{na}
\end{aligned} \tag{E.1}$$

where

$$F_s = PC_r \frac{A}{M} \tag{E.2}$$

and P is the solar constant, C_r is the coefficient of radiation, A is the area of the satellite, M is the mass of the satellite, and r_i is the distance of the Sun and the Earth.

Appendix F. Perturbation Due to Zonal Harmonics

Zonal harmonics cause also secular and long-periodic motion in orbital elements. According to Vinti⁵⁾, perturbing functions are derived as follows using the techniques by Escobal²⁶⁾. Perturbing functions due to J_2 are following.

$$\begin{aligned}
 \dot{a} &= 0 \\
 \dot{e} &= 0 \\
 \dot{i} &= 0 \\
 \dot{\Omega} &= -\tilde{J}_2 n \cos i \\
 \dot{\omega} + \dot{\Omega} \cos i &= \tilde{J}_2 n \left(1 - \frac{3}{2} \sin^2 i\right) \\
 \dot{M}_0 + \sqrt{1-e^2} (\dot{\omega} + \dot{\Omega} \cos i) &= 2\tilde{J}_2 n \sqrt{1-e^2} \left(1 - \frac{3}{2} \sin^2 i\right)
 \end{aligned} \tag{F.1}$$

where

$$\tilde{J}_2 = \frac{3 J_2 a_e^2}{2 p^2} \tag{F.2}$$

Perturbing functions due to J_3 are following.

$$\begin{aligned}
 \dot{a} &= 0 \\
 \dot{e} &= \tilde{J}_3 n (1-e^2) \sin i \left(1 - \frac{5}{4} \sin^2 i\right) \cos \omega \\
 \dot{i} &= \tilde{J}_3 n e \cos i \left(1 - \frac{4}{5} \sin^2 i\right) \cos \omega \\
 \dot{\Omega} &= \tilde{J}_3 n e \cot i \left(1 - \frac{15}{4} \sin^2 i\right) \sin \omega \\
 \dot{\omega} + \dot{\Omega} \cos i &= \tilde{J}_3 n \frac{1+4e^2}{e} \sin i \left(1 - \frac{5}{4} \sin^2 i\right) \sin \omega \\
 \dot{M}_0 + \sqrt{1-e^2} (\dot{\omega} + \dot{\Omega} \cos i) &= 8\tilde{J}_3 n e \sqrt{1-e^2} \sin i \left(1 - \frac{5}{4} \sin^2 i\right) \sin \omega
 \end{aligned} \tag{F.2}$$

where

$$\tilde{J}_3 = \frac{3 J_3 a_e^3}{2 p^3} \tag{F.3}$$

Similarly, perturbing functions due to J_4 are derived as follows.

$$\begin{aligned}
\dot{a} &= 0 \\
\dot{e} &= \tilde{J}_4 n e (1 - e^2) (1 - 7 \cos^2 i) \sin^2 i \sin(2\omega) \\
\dot{i} &= 0 \\
\dot{\Omega} &= -\tilde{J}_4 n (2 + 3e^2) (3 - 7 \cos^2 i) \cos i \\
&\quad + 2\tilde{J}_4 n e^2 (4 - 7 \cos^2 i) \cos i \cos(2\omega) \\
\dot{\omega} + \dot{\Omega} \cos i &= -\tilde{J}_4 n \left(1 + \frac{3}{4} e^2\right) (3 - 30 \cos^2 i + 35 \cos^4 i) \\
&\quad + \tilde{J}_4 n \left(1 + \frac{5}{2} e^2\right) (1 - 8 \cos^2 i + 7 \cos^4 i) \cos(2\omega)
\end{aligned} \tag{F.3}$$

where

$$\tilde{J}_4 = \frac{15}{32} \frac{J_4 a_e^4}{p^4} \tag{F.4}$$